Article

Buried Depth of a Submarine Pipeline Based on Anchor Penetration

Xueyuan Zhu, Qinglong Hao * and Jie Zhang

Navigation College, Dalian Maritime University, Dalian 116026, China
* Correspondence: haoql@dlmu.edu.cn

check for updates

Abstract: Anchor penetration is an important issue involved in the study of submarine pipeline damage accidents. To explore the penetration of a ship's anchor under certain conditions, this study investigated the motion and force of an anchor and formulated a calculation method for the bottoming speed of an anchor. Meanwhile, the depth of anchor penetration was calculated under different conditions according to bottoming speed through programming. Finally, the reliability of the calculation method for the penetration depth was verified by comparing the actual measurement and the numerical simulation. On the basis of the findings, the calculation results were further analyzed, and conclusions were derived regarding the relationship between anchor mass, the horizontal projected area of the anchor, the anchor height on the water surface, and water depth. The conclusions provide suggestions for the application of anchor penetration in terms of seabed depth with certain reference values.

Keywords: submarine pipeline; anchoring; bottoming speed; penetration

1. Introduction

As humans continuously develop and utilize marine resources, the submarine pipeline network has become increasingly dense in nearshore or archipelagic areas where the level of human activities is high. Simultaneously, the risk of submarine pipeline damage caused by human activities has increased. Statistics indicate that the majority of submarine pipeline damage accidents that occurred worldwide in recent years have been caused by human factors. Improper anchorage accounts for a considerable proportion of these accidents.

The damage caused by improper anchorage to submarine pipelines includes two types: impact and drag damages. If a submarine pipeline is located below the anchor point while a ship is anchoring, then the anchor may directly hit the pipeline when it penetrates into the seabed. Occasionally, the mooring point may be located near a submarine pipeline. The anchor may also hit the pipeline when it is dragged or weighed. These scenarios may cause submarine pipelines to shift and deform, thereby reducing their service life, or more seriously, they may result in the disruption and rupture of pipelines, thereby causing major economic losses and even marine pollution. Accordingly, a quantitative analysis should be conducted of the anchoring penetration depth of a ship to effectively reduce and prevent submarine pipeline damage caused by improper anchorage. To maintain the performance of submarine pipelines and ensure the safety of the marine environment, the anchor penetration depth and a reasonable submarine pipeline depth should be determined based on varying water depths, seabed geologies, and anchor weights.

In terms of anchor penetration, our predecessors have made a large number of contributions. Japanese scholars have carried out actual anchor dropping experiments on merchant ships' common anchors and obtained the measured values of anchor penetration under certain anchoring conditions [1]. Kim et al. proposed a rational analytical embedment model, based on strain rate-dependent shearing

resistance and fluid mechanics drag resistance to predict the embedment depth in the field [2]. They also adopted the large deformation finite-element (LDFE) method to analyze the behavior of a torpedo anchor during dynamic installation in two-layered non-homogeneous clay sediments, and proposed an extended total energy-based method to assess the anchor embedment depth in two-layered fine-grained ocean sediments [3]. Wang et al. conducted several penetration experiments and proposed a formula calculating the penetration depth in soft wet soil [4]. Wang experimentally investigated the penetration depth of a torpedo anchor in a two-layered soil bed and proposed an empirical formula to predict the penetration depth of a torpedo anchor in a two-layered soil bed [5]. Liu et al proposed a numerical framework to predict the embedment depth of gravity installed anchors (GIAs), considering the effects of soil strain rate, soil strain-softening, and hydrodynamic drag [6]. Zhao et al. developed a numerical approach incorporating anchor line effects to calculate the penetration of drag anchors based on the coupled Eulerian–Lagrangian method [7]. Moreover, they proposed fitted formulae to quickly evaluate the penetration of gravity installed anchors in clay [8]. Gao et al. have a deeper understanding of anchor penetration in the seabed. They experimentally, numerically, and theoretically analyzed the anchor penetration process and proposed a prediction method for the average bearing coefficient, which takes into account soil deformation, effects of strain and strain rate, effect of the touch-down velocity, as well as a prediction method for anchor penetration depth in clays [9]. However, previous research has mostly focused on the specific types of anchorage and seabed geology, but few researchers have considered the diversity and complexity of the seabed geology in practical engineering. Therefore, the purpose of this paper is to put forward a relatively fast method for predicting anchor penetration under complex geological conditions, which has a high reference value for the depth discussion of buried pipes in practical engineering.

A ship's anchoring process is divided into two stages, namely dropping the anchor into the water and seabed penetration, to improve the understanding of the mechanism of anchor damage to submarine pipelines. For a certain type of anchor and submarine bottom, the bottoming speed of the anchor will determine its kinetic energy. When the kinetic energy is high, the penetration depth will be large. First, the movement of the anchor in the water should be simulated to obtain its bottoming speed. Then, the anchor's motion during penetration should be analyzed, and the penetration depth should be calculated based on the simulation result of the anchor's bottoming speed. Finally, the penetration depth can be reasonably predicted under different conditions by changing the simulation conditions. The results can provide a reference for analyzing anchoring accidents.

2. Calculation of Bottoming Speed

2.1. Analysis of Factors that Affect the Dropping Speed of an Anchor

From practical experience, an anchor falling in the water will be subjected to gravity, the buoyancy and resistance of seawater, anchor chain tension, and seawater flow. Among these factors, gravity, buoyancy, and resistance of seawater are the major forces experienced by the anchor during its movement. Given that anchoring focuses on the vertical movement of the anchor, and the temperature and density of seawater have minimal effect on the anchor's movement, the flow, density, and temperature of seawater can be disregarded as secondary factors [10].

The anchor will inevitably drive the chain's movement when it falls because the end of the chain is not free. Based on previous data [1], when the anchor reaches a certain depth below the water surface, the dropping speed of the anchor's chain will be close to the final speed of the anchor falling without a chain. Figure 1 shows the schematic of an anchor's dropping speed with and without a chain obtained from anchoring test data. As shown in the figure, the speed difference of an anchor with a certain mass with or without a chain gradually decreases with an increase in water depth. The speed tends to be consistent when the water depth is sufficiently deep. Therefore, the anchor speed can be calculated without considering the influence of the chain on the anchor.
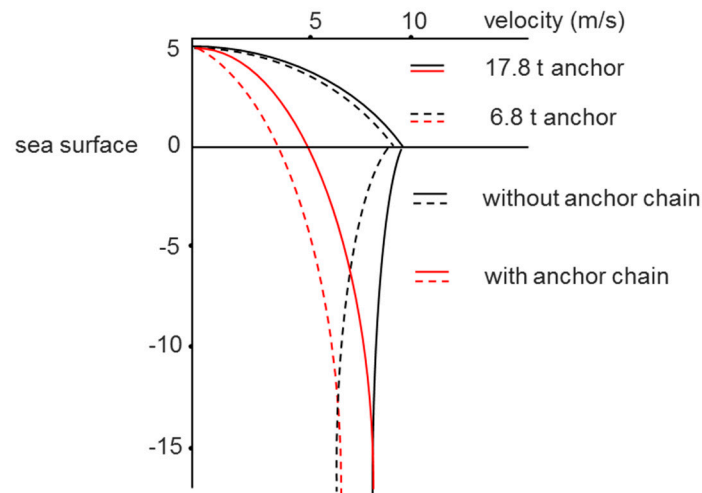
Figure 1. Falling speed of an anchor with and without a chain.

The scale parameters of several typical rodless anchors are obtained according to statistical data [11], and the fitting curves of A_f and A_S with M are established as shown in Figure 2. The combined determination coefficient R^2 is 0.999, with a high fitting degree.
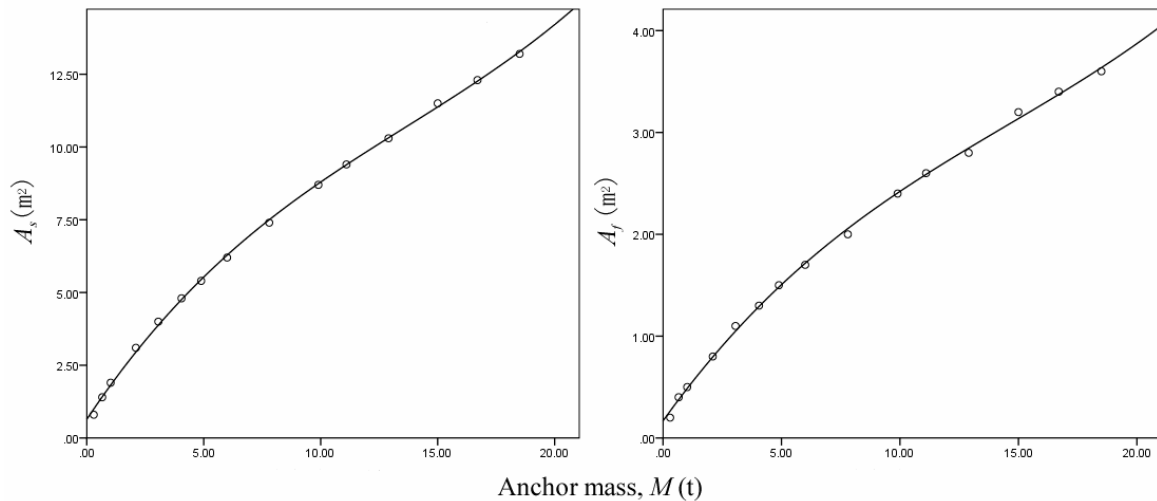

Figure 2. Fitting relationship of A_f and A_s with M.

In accordance with the preceding relationship, the fitting equations for A_f and A_s are approximately derived from the anchor's mass, M, as shown in Equations 1 and 2. A_f and A_s, respectively, represent the horizontal projected area and the lateral area of the anchor (m^2).

$$A_f = 0.1678 + 0.3247 \times M + (-0.0129) \times M^2 + 0.0003 \times M^3; \tag{1}$$

$$A_s = 0.6408 + 1.2032 \times M + (-0.0513) \times M^2 + 0.0013 \times M^3. \tag{2}$$

2.2. Dropping Speed of the Anchor in the Water

The force analysis of the anchor dropping process is illustrated in Figure 3. As shown in the figure, the coordinate system uses the sea level as the coordinate origin and the downward direction as the positive direction. The anchor is only affected by gravity, buoyancy, and drag force, whereas other factors are ignored.
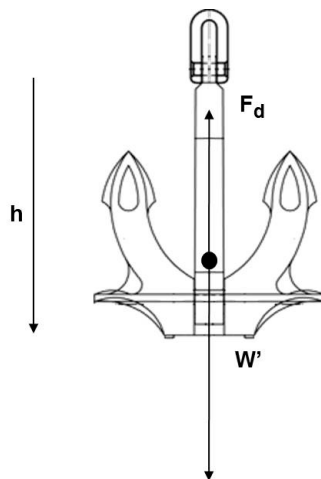
Figure 3. Force analysis of an anchor in the water.

When an object falls in seawater, resistance increases with an increase in speed and stabilizes to a certain value when it reaches a particular degree. Resistance is calculated according to the resistance around the flow as follows [12,13]:

$$F_d = \frac{1}{2}C_D\rho_w A_f v^2 \tag{3}$$

From the balance formula, we derive

$$W' - \frac{1}{2}C_D\rho_w A_f v^2 = 0 \tag{4}$$

$$W' = Mg - \rho_w Ug \tag{5}$$

$$U = \frac{M}{\rho_a} \tag{6}$$

where W' is the floating capacity of anchor (N); M is the anchor mass (kg); g is the gravitational acceleration (9.81 m/s^2); ρ_a is the anchor density (kg/m^3); ρ_w is the seawater density (kg/m^3); U is the anchor volume (m^3); F_d is the seawater resistance (N); C_D is the resistance coefficient; and v is the anchor speed (m/s).

An anchor typically reaches the final degree v_s when water depth is sufficient [14].

$$v_s = \sqrt{\frac{2Mg(1 - \rho_w/\rho_a)}{A_f \rho_w C_D}} \tag{7}$$

Considering that the anchor is thrown from a ship, the relationship between the speed and depth of the anchor in the water is obtained by analyzing the force before anchoring and the force in the water. In this manner, the speed of the anchor can be obtained at any water depth [15].

Assume that the anchor is moving in still water when the ship is anchored. Then, the following equation is obtained according to Newton's second law of motion:

$$(M + M_a)\frac{dv}{dt} = W' - F_d \tag{8}$$

Substituting Equation (3) into Equation (8) results in

$$(M + M_a)\frac{dv}{dt} = Mg(1 - \frac{\rho_w}{\rho_a}) - \frac{1}{2}C_D\rho_w A_f v^2 \tag{9}$$

The anchor is thrown from a position with height h_0 above the water surface. In accordance with the velocity formula of free-falling motion, the initial conditions are expressed as

$$v|_{h=0} = \sqrt{2gh_0} \qquad (10)$$

where M_a is the additional quality, $M_a = 2M_s = 2\rho_w U$; t is the moving time of the anchor under water; h is the displacement of the anchor under water (m); and v is the velocity (m/s) at which the displacement of the anchor is h under water.

Given that

$$\frac{dv}{dt} = \frac{dv}{dh} \cdot \frac{dh}{dt} = v\frac{dv}{dh} \qquad (11)$$

Equation (9) can be written as

$$(M + M_a)v\frac{dv}{dh} = Mg(1 - \frac{\rho_w}{\rho_a}) - \frac{1}{2}C_D\rho_w A_f v^2 \qquad (12)$$

Considering h as a function of v, $h = h(v)$. Equation (12) is written as

$$\frac{dh}{dv} = \frac{(M + M_a)v}{Mg(1 - \frac{\rho_w}{\rho_a}) - \frac{1}{2}C_D\rho_w A_f v^2} \qquad (13)$$

The initial conditions are expressed as

$$h\Big|_{v=\sqrt{2gh_0}} = 0 \qquad (14)$$

Then, $h = h(v)$ is obtained as

$$h = \frac{(\rho_a U + 2U\rho_w) \cdot \text{In}(2gU\rho_w - 2\rho_a U + 2C_D A_f gh_0\rho_w)}{C_D A_f \rho_w} \\ - \frac{(\rho_a + 2U\rho_w) \cdot \text{In}(C_D A_f \rho_w v^2 - 2\rho_a gU + 2gU\rho_w)}{C_D A_f \rho_w} \qquad (15)$$

After processing, $h = h(v)$ is converted to $v = v(h)$.

$$v = \sqrt{2g\left[\left(h_0 - \frac{U}{C_D A_f} \cdot \frac{(\rho_a - \rho_w)}{\rho_w}\right) \cdot e^{-(\frac{C_D A_f \rho_w}{U(\rho_a + 2\rho_w)} \cdot h)} + \frac{U}{C_D A_f} \cdot \frac{(\rho_a - \rho_w)}{\rho_w}\right]} \qquad (16)$$

Using Equation (16) and the combination with the given anchor parameters, the velocity of the anchor can be obtained at any displacement h under the water, whereas the anchor's bottoming speed can be obtained according to water depth condition.

The measured data of a set of anchor bottoming speeds are compiled based on foreign literature on anchoring experiments [1]. Equation (16) is used to calculate the velocity of the anchor under the same conditions. The two values are relatively close, with an error of less than 20%. The calculated value is slightly higher than the measured value, which is relatively safe for determining the submarine pipeline depth by calculating the penetration depth. The anchor bottoming speed method used in this study is reasonable. The detailed results are presented in Table 1.

Table 1. Comparison of calculated and measured bottom speeds.

No.	Anchor Mass (t)	Horizontal Projection Area of Anchor (m^2)	Aerial Altitude (m)	Water Depth (m)	Measured Speed (m/s)	Calculated Speed (m/s)	Error
1	17.8	3.5	6.3	19.5	8.2	8.47	3.3%
2	17.8	3.5	5	19.5	8	8.43	5.4%
3	16.1	3.3	5	17.2	7.6	8.28	8.9%
4	16.1	3.3	2.5	17.2	7.2	8.19	13.8%
5	16.1	3.3	0	17.2	6.9	8.09	17.2%
6	6.84	1.9	6.5	17	6.9	7.12	3.2%
7	6.84	1.9	3.4	17	6.8	7.07	4.0%
8	6.84	1.9	0	17	6	7.01	16.8%
9	1.26	0.6	1.6	17.7	4.5	5.39	19.8%
10	1.26	0.6	0	17.7	4.5	5.39	19.8%

2.3. Discussion of Anchor Bottoming Speed

From the preceding analysis, the anchor bottoming speed is largely affected by anchor mass *M*, anchor plane projected area A_f, aerial altitude h_0, and water depth *H*. Therefore, the relationship between the anchor bottoming speed and the aforementioned independent variables was calculated and analyzed using the bottoming speed calculation model derived in this study.

(1) Quality of anchor *M*

To evaluate the influence of anchor mass *M* on bottoming speed, anchors with different masses (M = 17.8, 16.1, 6.8, and 1.3 t) were used to determine the relationship between the velocity and displacement of an anchor under water *h* at the same aerial altitude (h_0 = 10 or 0 m), as shown in Figure 4.
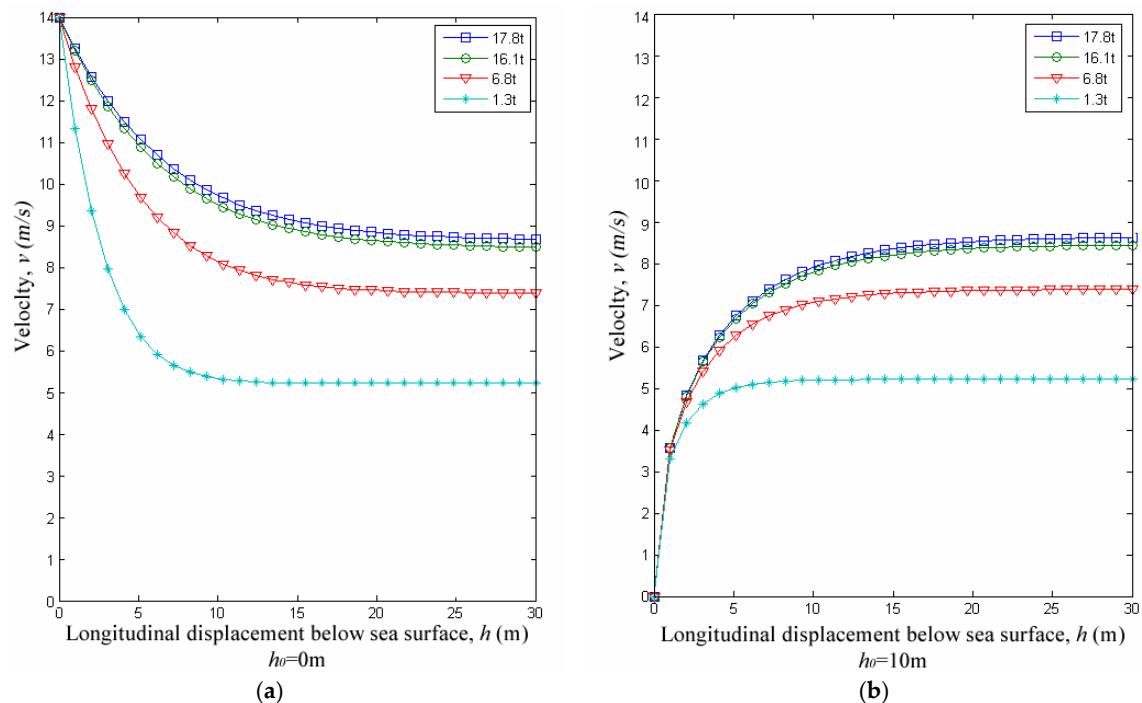

Figure 4. Falling speeds of anchors with different masses ((**a**) at altitudes of 0 and (**b**) at altitudes of 10 m).

Therefore, for the determined anchor height and water depth conditions in the case where the air altitude h_0 is the same, the bottoming speed will be faster when the anchor mass is larger.

(2) Horizontal projected area A_f

Three anchors with a mass of 17.8 t were used, and their A_f values were assumed as 3.2, 3.6, and 4.0 m^2. The anchoring situations at 10 and 0 m were calculated, and the result is shown in Figure 5.
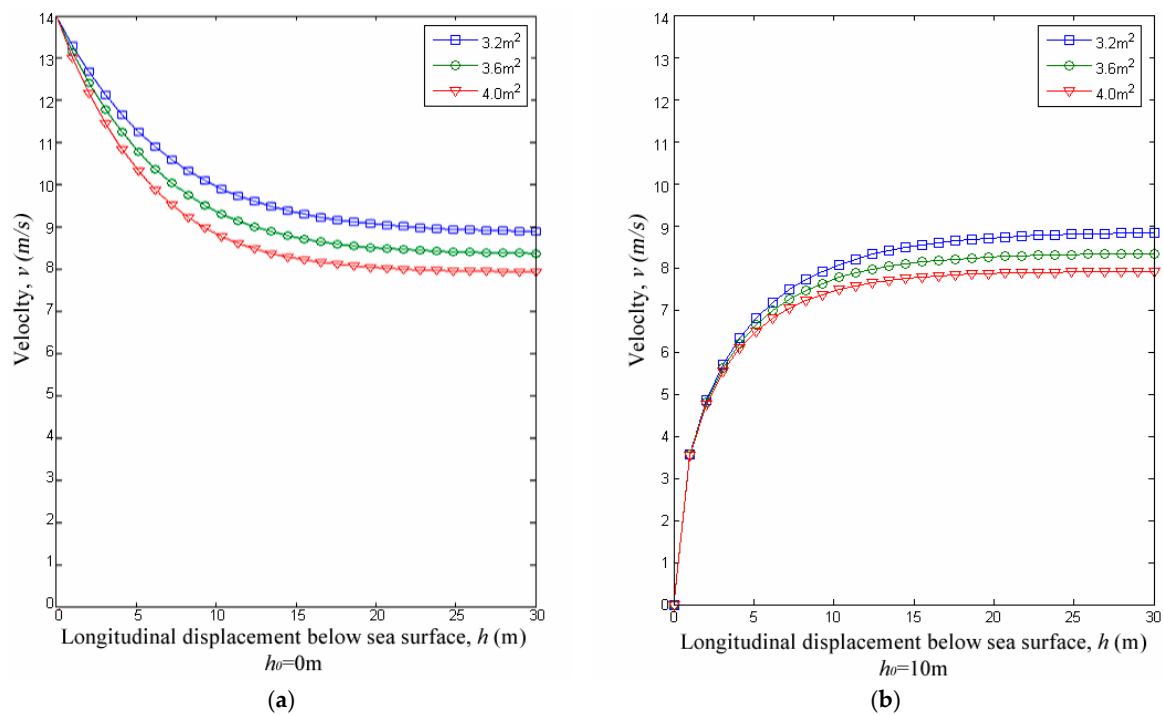

Figure 5. Falling speeds of anchors with different horizontal plane projected areas ((**a**) at altitudes of 0 and (**b**) at altitudes of 10 m).

Therefore, when the aerial altitude h_0 is the same under the same anchor height and water depth conditions, the smaller the A_f value, the faster the bottoming speed.

(3) Aerial altitude h_0

Assume a 17.8 t anchor at four different altitudes h_0 (10, 5, 2, and 0 m). The relationship between anchor speed and anchor displacement under the water was calculated, and the result is shown in Figure 6.
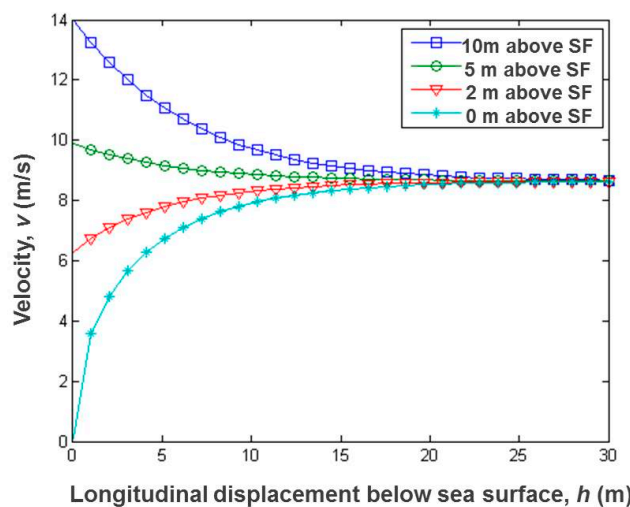

Figure 6. Anchor speed while anchoring at different altitudes.

When the water is shallow (i.e., below 10 m), the bottoming speed of the anchor will be faster at a higher aerial altitude h_0. When the water depth increases to a certain value (i.e., approximately 15 m),

altitude h_0 exerts less influence on the bottoming speed of the anchor. When the water is sufficiently deep (i.e., more than 20 m), the influence of aerial altitude h_0 on the bottoming speed of the anchor is no longer evident.

(4) Water depth H

As shown in Figure 6, when the aerial altitude h_0 is low (i.e., 0–2 m), the falling speed of the anchor will increase with depth. When h_0 is high (i.e., 5–10 m), the falling speed of the anchor will continue to decrease as depth increases. When the anchor sinks to a certain depth, its sinking speed will no longer change considerably with an increase in water depth, and the final bottoming speed will approach a certain value. When the water is sufficiently deep, the ultimate bottoming speed of the anchor is negligible due to the effect of water depth on anchoring h_0.

3. Calculation of Submarine Penetration Depth

3.1. Calculation Model for Submarine Penetration Depth

After anchoring into the seabed soil, the anchor's speed is reduced from the bottoming speed to zero. Therefore, the relationship between speed and penetration depth can be established. The penetration depth can be obtained when the speed of the anchor is reduced to zero.

The dynamic analysis of the anchor penetration process is shown in Figure 7. The earth-moving process primarily considers the effective gravity and resistance of an object. Under the combined actions of upward resistance and downward gravity, an anchor exhibits a decelerating motion until it stops [16]. The effective gravity is calculated based on floating capacity, and resistance comprises end bearing, side friction, and dragging [17].
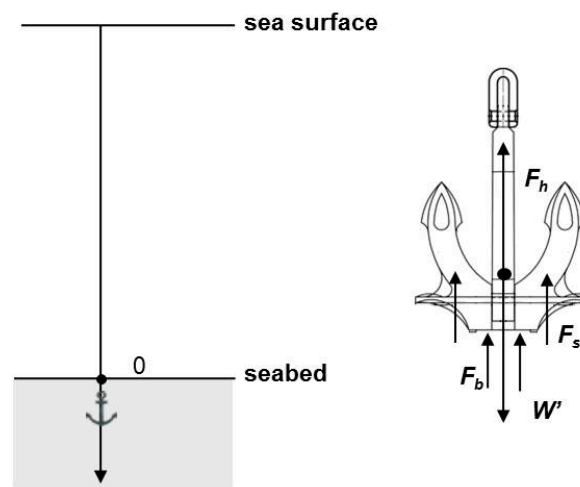

Figure 7. Force analysis of an anchor in soil.

The equation for the anchor's motion in the seabed soil is established according to Newton's second law of motion as follows:

$$M^* \frac{dv}{dt} = W' - F(v, z) \tag{17}$$

$$F(v, z) = F_b(v, z) + F_s(v, z) + F_h(v) \tag{18}$$

where M^* is the total mass (kg), which equals the sum of anchor mass M and the momentum additional mass $2M_s$ (i.e., $M^* = M + 2M_s$ [9]); W' is the effective weight of the anchor (N); F_b is the end-bearing resistance (N); F_s is the side-frictional resistance (N); and F_h is the dragging resistance (N).

The penetration depth during the anchoring process is highly dependent on substrate quality. To calculate the penetration depth, the seabed sediment is typically divided into clay and sand. "Clay" includes sandy clay, clay, mud, and silt. "Sand" includes sand and mixed sediments with a large amount of sand.

The considerable differences in the properties of clay and sand can affect the end-bearing resistance and side-frictional resistance of an anchor [18]. Therefore, when calculating the anchor penetration depths in clay and sand, the calculation formulae for end-bearing resistance and side-frictional resistance adopt different forms [19,20]. The end-bearing, side-frictional, and dragging resistances of clay are expressed as follows [17]:

$$F_b(v,z) = S_e S_u N_c A_f \tag{19}$$

$$F_s(v,z) = \delta \cdot S_e \frac{S_u}{S_t} A_s \tag{20}$$

$$F_h = \frac{1}{2} C_d \rho_s A_f v^2 \tag{21}$$

The formulae for end-bearing resistance and side-friction resistance in sand are different, as follows:

$$F_b(v,z) = S_e k P_0 \tan\varphi A_f = 0.8 S_e (\rho_s - \rho_w) g \cdot z \cdot \tan\varphi A_f \tag{22}$$

$$F_s(v,z) = \delta S_e P_0 N_q A_s = \delta S_e (\rho_s - \rho_w) g \cdot z \cdot N_q A_s \tag{23}$$

where ρ_s is the density of seabed soil (kg/m^3); N_c is the ultimate bearing capacity of soil [21]; S_u is the undrained shear strength of soil (kPa); S_t is the soil sensitivity; S_e is the high-speed shear strain coefficient of soil; δ is the anchor side high-speed viscosity coefficient; φ is the internal friction angle of soil; and $N_q \approx 105 \tan^2 \varphi$ [21].

For sand, $\frac{S_e^*}{S_e} = 1$, where S_e^* is the maximum shear strain coefficient, and its value is fixed for a certain type of clay.

For clay, the relationship between S_e and S_e^* is [17]

$$\frac{S_e^*}{S_e} = \left[1 + \frac{1}{\sqrt{\frac{C_e v}{S_u l} + C_0}} \right] \tag{24}$$

where v is the speed of the anchor when entering the soil (m/s); l is the length of the anchor when entering the soil (m); C_0 is a constant with a value of 0.04; and C_e is a constant with a value of 980 N/m^2·s.

Four typical clays and three typical sands were used in the calculation. The physical parameters used in the calculation are provided in Table 2 [22].

Table 2. Physical parameters used in the calculation.

Type	Name	Density	Undrained Shear Strength	Saturation Severity	Maximum Shear Strain Coefficient
Clay	Silt	1400	<5	16.1	4.0
	Slime	1500	<15	18.2	3.8
	Soft clay	1550	10–20	19.5	3.7
	Hard clay	1700	>20	22.0	3.4
Sand	Loose sand	1650	20	20.3	3.6
	Medium sand	1800	27	21.6	3.4
	Dense sand	2000	35	22.6	3.2

3.2. Numerical Calculation Method for Seabed Penetration

From Equation (17), we derive

$$\frac{dv}{dt} = \frac{W' - F(v,z)}{M^*} \tag{25}$$

because

$$\frac{dv}{dt} = \frac{dv}{dz} \cdot \frac{dz}{dt} = v\frac{dv}{dz} \tag{26}$$

Therefore,

$$v\frac{dv}{dz} = \frac{W' - F(v,z)}{M^*} \tag{27}$$

When Δv_i and Δz_i are sufficiently small, the following can be derived from the preceding formula:

$$v_{i+1} = v_{i-1} + \left[\frac{W'}{M^* v_i} - \frac{F_b(v_i, z_i) + F_s(v_i, z_i)}{M^* v_i} - \frac{F_h(v_i)}{M^* v_i} \right] \cdot 2\Delta z \tag{28}$$

In Equation (28), v_{i+1} is the value obtained and calculated by using an iterative method. If v_{i+1} is greater than 0, then the anchor continues to drop into the seabed and increases by z_i. Until v_{i+1} becomes less than 0, the value of z at the second time is the depth of the anchor that penetrates into the seabed soil (i.e., the penetration depth).

4. Numerical Simulation of Submarine Penetration

4.1. Numerical Simulation Method

A 10 t anchor was used as an example. The anchor's mass (10 t), horizontal projected area (2.4 m^2), side area (8.8 m^2), and initial aerial altitude (2 m) were inputted along with water depth (12 m) and soil type (ooze). The output is shown in Figure 8.
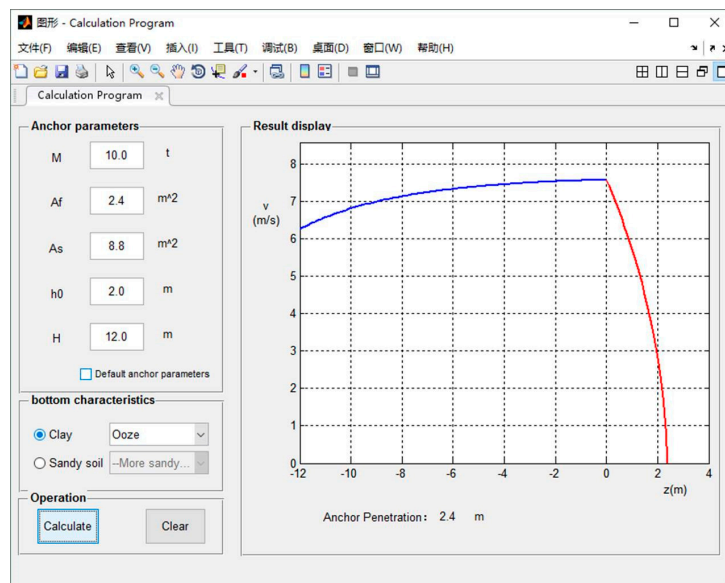

Figure 8. Calculation example.

The blue line in the result is in the negative direction of the abscissa z, which indicates the velocity curve of the anchor while falling in the water. The red line in the positive direction of z indicates the velocity curve of the anchor in the soil. The resulting penetration was 2.4 m.

4.2. Discussion and Evaluation of the Simulation Results

The penetration depth can be obtained based on the anchoring and bottom elements by using the aforementioned calculation method. To verify the accuracy of the theoretical calculation of penetration depth, the literature can be used to obtain the measured penetration data of rodless anchoring experiments [1,23–29]. The measured values were classified and sorted, and the statistical values of

the two sets of measured penetration depths, as shown in Tables 3 and 4, were used as bases to verify the calculated values.

Table 3. Penetration depth in clay substrate from anchoring experiments.

No.	Anchor Mass (t)	Substrate	Measured Penetration Depth (m)
1	0.5	Silt	1.88
2	1	Silt	2.00
3	2	Silt (with sand)	1.52
4	2.5	Ooze (with stiff clay below)	1.81
5	3	Silt	2.30
6	3.41	Silt (with sand)	1.32
7	6	Mud	1.91
8	8	Silt	2.20
9	9.7	Silt	3.03
10	18	Silt (with sand)	2.63

Table 4. Penetration depth in sand substrate from anchoring experiments.

No.	Anchor Mass (t)	Substrate	Measured Penetration Depth (m)
1	0.5	Sand	0.05
2	1	Sand	0.45
3	1.5	Sand	0.75
4	1.75	Sand (with mud)	0.25
5	3.4	Sand	0.34
6	8.8	Sand soil	0.90
7	12.5	Sand (with mud)	0.84
8	14.8	Sand soil	1.64
9	18.8	Sand soil	0.71
10	20	Sand soil	1.93
11	20.9	Sand soil	1.75

The penetrations of anchors with different masses in seven typical sediments (three clays and four sands) were calculated using the calculation model of falling anchor penetration developed in this study. The calculation of the anchor's bottoming speed was considered in the case with sufficient water depth. The comparison between the measured and calculated values is provided in Tables 5 and 6.

Table 5. Penetration depth of the anchor in clay substrate.

No.	Anchor Mass (t)	Measured Penetzration Depth (m)	Calculated Penetration Depth (m)			
			Silt	Ooze	Soft Clay	Hard Clay
1	0.5	1.88	1.3	1	0.9	0.7
2	1	2.00	1.6	1.2	1	0.9
3	2	1.52	1.9	1.5	1.3	1.1
4	2.5	1.81	2.1	1.6	1.4	1.3
5	3	2.30	2.3	1.8	1.6	1.4
6	3.41	1.32	2.4	1.8	1.6	1.4
7	6	1.91	2.7	2.1	1.8	1.6
8	8	2.20	2.9	2.2	2	1.8
9	9.7	3.03	3.0	2.4	2.1	1.9
10	18	2.63	3.7	2.9	2.6	2.3

Table 6. Penetration depth of the anchor in sand soil substrate.

No.	Anchor Mass (t)	Measured Penetration Depth (m)	Calculated Penetration Depth (m)		
			Loose Sand	Medium Sand	Dense Sand
1	0.5	0.05	0.5	0.4	0.3
2	1	0.45	0.7	0.5	0.4
3	1.5	0.75	0.8	0.7	0.5
4	1.75	0.25	0.8	0.7	0.5
5	3.4	0.34	1.0	0.8	0.7
6	8.8	0.90	1.4	1.1	0.9
7	12.5	0.84	1.6	1.3	1.1
8	14.8	1.64	1.7	1.4	1.1
9	18.8	0.71	1.8	1.5	1.2
10	20	1.93	1.8	1.5	1.2
11	20.9	1.75	1.8	1.5	1.3

The calculated penetration depth of an anchor with the same mass can constitute a range because the calculations are based on different substrates. The two sets of data were processed separately, and the high–low graph of the penetration depth in the clay and sand substrates is shown in Figure 9, which was used to determine whether the measured value was within the range of the calculated value. The red cross in the figure indicates the penetration depth obtained in the anchoring test. The upper and lower ends of the high and low line segments that correspond to the mass of each anchor are the maximum and minimum values calculated for the penetration depth in different types of clay or sand.
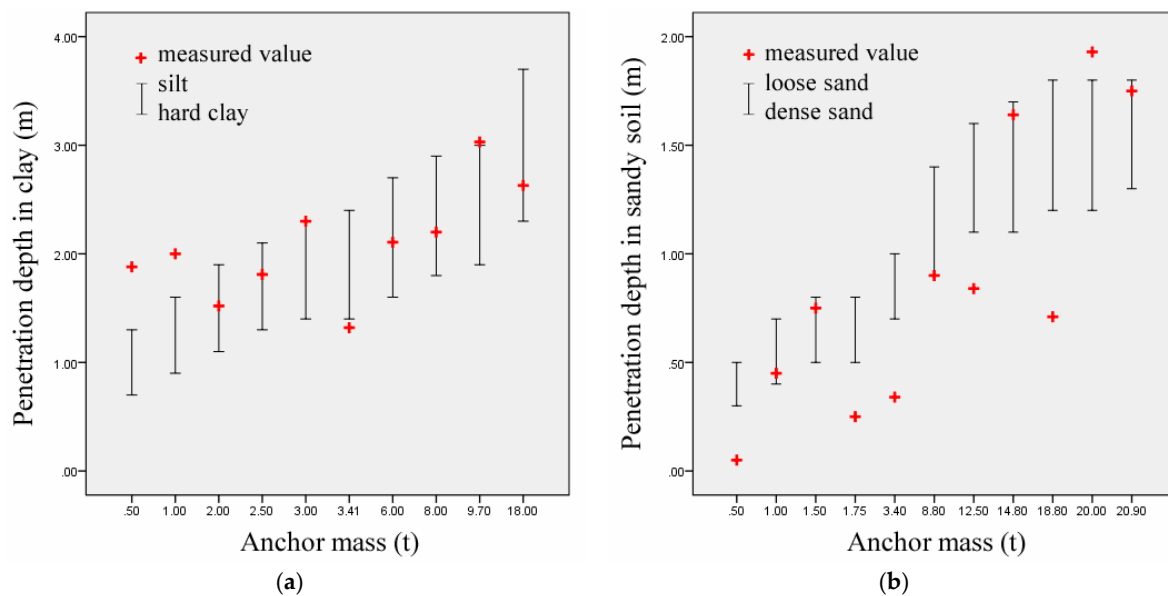

Figure 9. High–low graph of the penetration depth ((**a**) in clay and (**b**) in sand substrates).

The analysis of the two datasets shows the following:

(1) The distribution of most measured values was within the range from the maximum to minimum of the calculated values, which indicates that most of the calculated values of the penetration depths were in good agreement with the measured data.

(2) When the substrate was sand, the measured value was lower than that of the minimum value of the calculated value, whereas the calculated value was higher than that of the measured value. This result is acceptable for protecting submarine pipelines.

(3) The individual measured values were higher than that of the maximum calculated value within the allowable range of error.

Based on the preceding analysis, the calculation of the anchoring penetration depth in this study exhibited certain rationality and credibility.

4.3. Prediction Formula for Penetration Depth

From the perspective of submarine pipeline protection, the buried depth standard will be safe when a large penetration depth is used as the basis for the buried depth of pipelines; that is, the calculated value being higher than the actual penetration depth tends to be safe. The overall analysis of the measured and calculated values of the aforementioned penetration was conducted, and the higher number between the two values was used for fitting to obtain the approximate relationship between the maximum penetration depth and the anchor mass, which can be used as a reference in applications.

Figures 10 and 11 show the scatterplots of the measured and calculated values for the penetration depth in clay and sand, respectively. The red circle represents the maximum measured and calculated values for the same penetration depth.
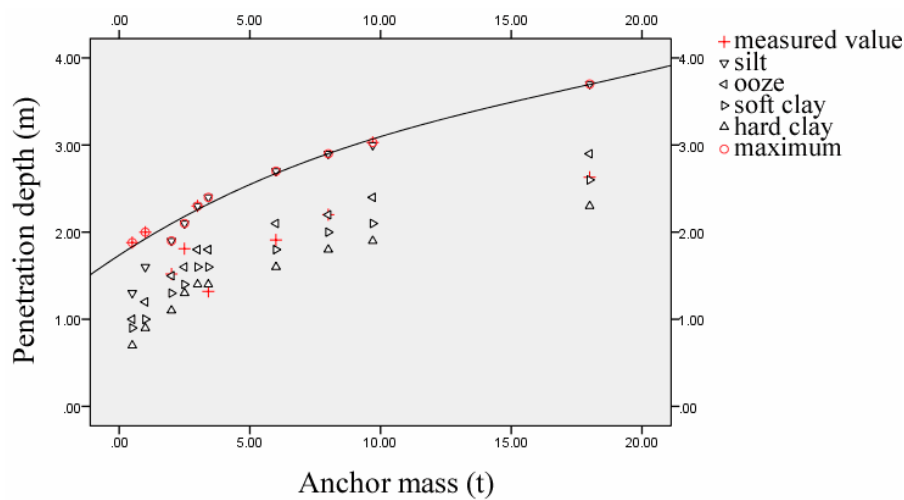

Figure 10. Scatterplot and regression curve of clay substrate penetration data (the measured values are from).
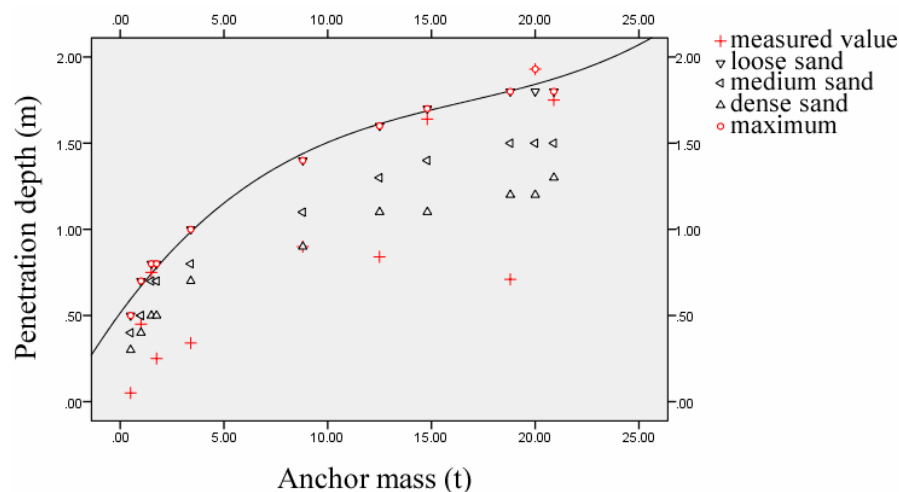

Figure 11. Scatterplot and regression curve of sand substrate penetration data (the measured values are from).

By comparing the calculated value with the measured value, it was found that the measured value under the clay condition was mostly distributed within the range of the maximum value and the minimum value, indicating that the calculated value and the measured value under the clay condition

have a good consistency. However, under the condition of sandy soil, some measured values were lower than the minimum value of calculated values, which may result from the composition of sandy soil being more complex, and the fitting in this paper was the maximum value of measured values and predicted values, so this result has good safety in the protection of submarine pipelines.

Based on the fitting goodness of each model, the model test results, and other related indicators, the most suitable curve model was used to perform the nonlinear regression of various curve models on the anchor's mass and the corresponding maximum penetration depth. The fitting indicates that the anchoring penetration curves of the two substrates can adapt to the regression fitting model of the cubic curve. Equations 29 and 30 are the regression equations for anchor penetration in clay and sand, respectively, which are fitted using a numerical method.

$$z = 1.736025 + 0.195281 \times M - 0.007310M^2 + 0.000140 \times M^3 \tag{29}$$

$$z = 0.514570 + 0.164297 \times M - 0.008163 \times M^2 + 0.000163 \times M^3 \tag{30}$$

A ship's anchor penetration under sufficient water depth can be effectively estimated using the aforementioned regression equation, which provides a basis for analyzing anchorage accidents in submarine pipelines and a reference for safe buried pipeline depths in submarine pipeline engineering.

5. Conclusions

In this study, the movement process of an anchor in water and when it penetrates seabed soil was analyzed based on relevant data, literature, and theories. A calculation method and program for penetration were then developed. The calculation results of penetration depth were verified based on the measured penetration data, which proved the credibility of the proposed calculation method for penetration depth. Furthermore, a regression equation for estimating the penetration depth of an anchor in actual, complex cases was proposed.

The main research results and conclusions of this study are summarized as follows:

(1) A calculation method for anchor bottoming speed was developed, and its relationships with anchor mass, horizontal projected area, the aerial altitude of the anchor above the water surface, and water depth were analyzed.

(a) The bottoming speed increased with an increase in anchor mass.

(b) The bottoming speed increased with a decrease in the projected area of the anchor's horizontal plane.

(c) The bottoming speed increased with an increase in the aerial altitude of the anchor. However, the bottoming speed was independent of altitude when the water was sufficiently deep.

(d) The bottoming speed of the anchor increased with an increase in water depth when the aerial altitude of the anchor was low. The bottoming speed of the anchor increased with an increase in water depth when altitude was high. The bottoming speed did not change with an increase in water depth when the water was sufficiently deep.

(2) A calculation method for anchor penetration depth was obtained by further utilizing the anchor's bottoming speed.

(3) A calculation program for penetration depth was designed using MATLAB. Combined with anchoring experimental data, the calculated penetration depth was verified to prove that the simulation method for penetration depth and the results obtained in this study exhibited good credibility.

(4) The approximate relationship between anchor mass and maximum penetration in clay and sand was obtained after data analysis and processing, considering the diversity and complexity of seabed soil composition in actual conditions. The result was safe to be used to estimate the penetration of an anchor with a certain mass in clay and sand. Thus, the findings of this study provide a reference for analyzing anchorage accidents in submarine pipelines and for determining the safe buried depth of submarine pipeline projects.

Under the condition of clay substrate, the predicted results of regression equation were in good agreement with the measured values. However, under the condition of sandy soil substrate, the prediction results of regression equation were obviously larger than the measured value, which is a limitation of this study, but is safe for the buried depth of submarine pipelines.

It is worth mentioning that with the development of Marine geological survey technology in the future, more and more attention will be paid to the accurate calculation of anchor penetration. Future studies should further analyze the accurate prediction of penetration under sandy soil substrate conditions to facilitate the application of anchor penetration to the buried depth of submarine pipelines.

Author Contributions: Conceptualization, X.Z.; Data curation, X.Z.; Formal analysis, X.Z.; Investigation, Q.H.; Methodology, Q.H.; Project administration, J.Z.

Conflicts of Interest: The authors declare no conflict of interest.

References

1. Port Technology Research Institute of Japan Transport Ministry. *The Penetration of Anchor in the Anchor Dropping Test*; Port Technology Research Institute of Japan Transport Ministry: Yokosuka, Japan, 1975.
2. Kim, Y.H.; Hossain, M.S.; Wang, D.; Randolph, M.F. Numerical investigation of dynamic installation of torpedo anchors in clay. *Ocean Eng.* **2015**, *108*, 820–832. [CrossRef]
3. Kim, Y.; Hossain, M.S.; Lee, J. Dynamic Installation of a Torpedo Anchor in Two-layered Clays. *Can. Geotech. J.* **2017**, *55*, 446–454. [CrossRef]
4. Wang, W.; Wang, X.; Yu, G. Penetration depth of torpedo anchor in cohesive soil by free fall. *Ocean Eng.* **2016**, *116*, 286–294. [CrossRef]
5. Wang, C.; Zhang, M.X.; Yu, G.L. Penetration Depth of Torpedo Anchor in Two-Layered Cohesive Soil Bed by Free Fall. *China Ocean Eng.* **2018**, *32*, 706–717. [CrossRef]
6. Liu, H.; Xu, K.; Zhao, Y. Numerical investigation on the penetration of gravity installed anchors by a coupled Eulerian–Lagrangian approach. *Appl. Ocean Res.* **2016**, *60*, 94–108. [CrossRef]
7. Zhao, Y.; Liu, H.; Li, P. An efficient approach to incorporate anchor line effects into the coupled Eulerian–Lagrangian analysis of comprehensive anchor behaviors. *Appl. Ocean Res.* **2016**, *59*, 201–215. [CrossRef]
8. Zhao, Y.; Liu, H. Toward a quick evaluation of the performance of gravity installed anchors in clay: Penetration and keying. *Appl. Ocean Res.* **2017**, *69*, 148–159. [CrossRef]
9. Gao, P.; Duan, M.; Gao, Q.; Jia, X.; Huang, J. A prediction method for anchor penetration depth in clays. *Ships Offshore Struct.* **2016**, *11*, 782–789. [CrossRef]
10. Li, Y.; Li, Y.; Hu, S. Numerical simulation of water entry of two-dimensional body. *J. Huazhong Univ. Sci. Technol.* **2011**, *12*, 46–49.
11. Lloyd's Register of Shipping. *Rules and Regulations for the Classification of Ships*; Lloyd's Register of Shipping: London, UK, 2004.
12. Shao, S.D. Incompressible SPH simulation of water entry of a free-falling object. *Int. J. Numer. Methods Fluids* **2009**, *59*, 91–115. [CrossRef]
13. Park, M.S.; Jung, Y.R.; Park, W.G. Numerical study of impact force and ricochet behavior of high speed water-entry bodies. *Comput. Fluids* **2003**, *32*, 939–951. [CrossRef]
14. Zhuang, Y.; Song, S. Study on the depth of submerged pipeline. *J. Dalian Marit. Univ.* **2013**, *1*, 61–64.
15. Hu, X.Z.; Liu, S.J. Numerical Simulation of Water Entry of Seafloor Mining Tool with Free Fall Motion. *Int. J. Fluid Mech. Res.* **2011**, *38*, 193–214.
16. Jairo, B.A.; Lima, J.C.; Machado, R.D. Torpedo Anchor Installation Hydrodynamics. *J. Offshore Mech. Arct. Eng.* **2006**, *128*, 286–293.
17. True, D.G. *Penetration of Projectiles into Seafloor Soils*; Civil Engineering Laboratory: Port Hueneme, CA, USA, 1975.
18. Kunitaki, D.M.; Lima, B.S.; Evsukoff, A.G. Probabilistic and Fuzzy Arithmetic Approaches for the Treatment of Uncertainties in the Installation of Torpedo Piles. *Math. Probl. Eng.* **2008**, *26*, 5–11. [CrossRef]

19. Liu, H.; Liu, C.; Yang, H. A novel kinematic model for drag anchors in seabed soils. *Ocean Eng.* **2012**, *49*, 33–42. [CrossRef]

20. Sriskandarajah, T. Assessment of Anchor Dragging on Gas Pipelines. In Proceedings of the Twelfth (2002) International Offshore and Polar Engineering Conference, Kitakyushu, Japan, 26–31 May 2002; pp. 26–31.

21. Xia, J. Soil Mechanics and Engineering Geology. Master's Thesis, Zhejiang University, Hangzhou, China, 2012.

22. Chen, X.; Ye, J. *Soil Mechanics Foundation*; Tsinghua University Press: Beijing, China, 2013.

23. Chen, X. Stability Analysis of Chunxiao Gas Field Group Submarine Pipeline. Master's Thesis, Zhejiang University, Hangzhou, China, 2004.

24. Allan, P.G.; Comrie, R.J. *Risk Assessment Methodology and Optimisation of Cable Protection for Existing and Future Projects*; Centre for Advanced Industry: Montecarlo, Monaco, 2004.

25. Allan, P.G.; Comrie, R.J. The Selection of Appropriate Burial Tools and Burial Depths. In Proceedings of the SubOptic 2001 International Convention, Kyoto, Japan, May 2001.

26. Allan, P.G.; Comrie, R.J. Selecting Appropriate Cable Burial Depths A Methodology. In Proceedings of the IBC Conference on Submarine Communications, Cannes, France, 26–28 October 1998; pp. 1–13.

27. Det Norske Veritas. *Risk Assessment of Pipeline Protection*; GCS: Oslo, Norway, 2010.

28. Dirk, L. Developments in anchor technology and anchor penetration in the seabed. In Proceedings of the Lecture on a Symposium on Installation of Submarine Power Cables for Grid Connection of Offshore Windparks, Bremen, Germany, March 2006; pp. 3–26.

29. Roderick, M. Ruinen Penetration Analysis of Drag Embedment Anchors in Soft Clays. In Proceedings of the Fourteenth (2004) International Offshore and Polar Engineering Conference, Toulone, France, 23–28 May 2004; pp. 531–542.